Thermodynamic Characterization of the Cooperativity of 40S Complex Formation during the Initiation of Eukaryotic Protein Synthesis†

Kay M. Parkhurst, Ronald E. Hileman, Debabrata Saha, Naba K. Gupta, and Lawrence J. Parkhurst*

Department of Chemistry, University of Nebraska—Lincoln, Lincoln, Nebraska 68588-0304

Received March 25, 1994; Revised Manuscript Received October 5, 1994⊗

ABSTRACT: The first step in mammalian protein synthesis is the formation of the 40S initiation complex, composed of the 40S ribosomal subunit (R), mRNA (M, here, a 10-mer oligoribonucleotide analogue containing the initiation codon), and the quaternary complex (Q, composed of eIF-2, GTP, Met-tRNA$_f^{Met}$, and the ancillary protein factor Co-eIF-2C). The interdependence of the binding of R, M, and Q in forming the 40S complex is currently unclear. We have determined the thermodynamic parameters that characterize these interactions. The binary constants for R + M and Q + M were determined spectroscopically, measuring changes in the anisotropy of the fluorescence emission of 3′-fluorescein labeled M. The other binary constant, for Q + R, and the ternary constant were determined from Millipore filtration assays using radiolabeled Met-tRNA$_f^{Met}$. The association constants for the binary reactions were as follows: K_a(Q,M) ≤ 0.14 × 10^6 M^{-1}, K_a(R,M) = 1.78 × 10^6 M^{-1}, and K_a(Q,R) = 0.94 × 10^6 M^{-1}. The binding of Q to R•M was markedly greater than that of Q to R [K_a(Q,R•M)/K_a(Q,R) > 62]. High cooperativity for this interaction occurs in either a single-site model or in lattice models for the binding of M to R. Data obtained using five other RNA 10-mers, each with the sequence altered at the AUG codon, suggest that this cooperativity is AUG dependent. The data are consistent with a scheme in which mRNA and Q bind independently to the 40S ribosome, but when the AUG codon is properly aligned with Q, a conformational change results in a 2.4 kcal/mol stabilization of the complex.

The first step in mammalian protein synthesis is the formation of a ternary complex between eukaryotic initiation factor 2,[1] Met-tRNA$_f^{Met}$, and GTP: eIF-2•GTP•Met-tRNA$_f^{Met}$. Subsequently, Met-tRNA$_f^{Met}$ is transferred to the 40S ribosomal subunit, and the Met-tRNA$_f^{Met}$•40S•mRNA initiation complex is formed. The interdependence of the binding of the three components of the initiation complex is currently unclear; data supporting significantly different views have been reported. The present consensus with respect to initiation complex formation, reviewed by Hershey (1991), can be summarized as follows: In eukaryotes, the ternary complex formed by eIF-2 binds to the 40S ribosomal subunit in the absence of mRNA. (This differs from the prokaryotic mechanism where mRNA is required for Met-tRNA$_f^{Met}$•40S formation.) Subsequently, several eIF-4 group proteins (eIF-4A, eIF-4B, and eIF-4F) bind to the 5′-cap site on mRNA and facilitate mRNA binding to the Met-tRNA$_f^{Met}$•40S complex. The Met-tRNA$_f^{Met}$•40S complex then scans the 5′-noncoding sequence in mRNA until it reaches the initiation codon. In contrast, Gupta and co-workers, using purified peptide chain initiation factors, demonstrated that Met-tRNA$_f^{Met}$ binding to the 40S ribosomal subunit was dependent on mRNA (Gupta et al., 1975; Roy et al., 1984, 1988). Their reports indicated that as in prokaryotes, Met-tRNA$_f^{Met}$ bound to 40S ribosomes by direct interaction with the internal initiation codon in mRNA. Consistent with these findings, several laboratories have now reported internal initiation with various viral and cellular mRNAs (Pelletier & Sonenberg, 1988; Jackson et al., 1990; Macejak & Sarnow, 1991; Hellen et al., 1993).

We have used a fractionated system to determine the thermodynamic parameters that characterize the interactions of the three components that comprise the initiation complex: 40S ribosomal subunits (R), mRNA (M), and quaternary complex (Q, the eIF-2•GTP•Met-tRNA$_f^{Met}$ ternary complex plus the ancillary protein factor Co-eIF-2C). The ancillary initiation factor Co-eIF-2C (which has eIF-3 and eIF-2B activities) is required to obtain appreciable amounts of ternary complex; we have therefore defined the quaternary complex, Q, as one of the three components of the 40S initiation complex. Binding constants were obtained for the three binary interactions, R + M, Q + R, and Q + M, and for the ternary interaction, Q + R + M. Once these values are known, the dependence of the binding of any two components on the third component is unambiguous, and there is sufficient information to quantitate cooperativity or "enhancement" in the three-component system. In the simplest model, the ratio of Q, R, and M in the 40S complex is 1:1:1. Since our mRNA analogue was a short oligonucleotide, we also considered multiple binding of M to R; the data were analyzed according to several schemes based on a lattice model in addition to the single-site model.

The mRNA analogues used in this study were 10-mer oligoribonucleotides. Analysis of nearly 700 published

† This work was supported by National Institutes of Health Research Grants GM 22079 (N.K.G.) and DK 36288 (L.J.P.).

* Author to whom correspondence should be addressed. Telephone: (402) 472-3316; Fax: (402) 472-9402; e-mail address: lparkhurst@unlinfo.edu.

⊗ Abstract published in *Advance ACS Abstracts,* November 15, 1994.

[1] Abbreviations: eIF, eukaryotic initiation factor; GMP−PNP, 5′-guanylyl imidodiphosphate; DTT, dithiothreitol; BSA, bovine serum albumin; DEPC, diethylpyrocarbonate; THF, tetrahydrofuran; TEAA, triethylammonium acetate; Tris, tris(hydroxymethyl)aminomethane; M, a 10-mer oligoribonucleotide, 5′-GAAGAUGGAA-3′; M*F, 3′-end fluorescein labeled M; R, 40S ribosomal subunits; Q, quaternary complex, either (eIF-2•GTP•Met-tRNA$_f^{Met}$•Co-eIF-2C) or (eIF-2•GMP-PNP•Met-tRNA$_f^{Met}$•Co-eIF-2C).

0006-2960/94/0433-15168$04.50/0 © 1994 American Chemical Society

eukaryotic mRNAs showed a consensus sequence around the initiating AUG codon to be 5′-GCCGCCACCAUGG-3′ (Kozak, 1987a). Changes in these flanking sequences usually result in a loss of translational efficiency (Kozak, 1987a), particularly in the positions −6 to −1 and +4, where the A of AUG is defined as +1 and numbering is from 5′ to 3′ without a zero position. The most pronounced loss of translational efficiency occurs when the −3 and +4 positions are altered. Thus messenger RNAs have been designated as "strongly" or "weakly" translated by considering only the −3 and +4 positions (Kozak, 1986, 1987b). The AUG-containing RNA 10-mer used for this study was therefore designed to include the −3 A and the +4 G without a stop codon (UGA, UAA, or UAG) in any reading frame and to have no significant inter- or intramolecular complementarity. Our primary goal was to quantitate the interdependence of R, M, and Q binding to form the initiation complex. However, we also investigated the AUG codon dependence of these cooperative interactions. Five additional RNA 10-mers were synthesized, which were modified to disrupt to AUG codon, and binding data were obtained for the ternary interaction using each of these analogues.

EXPERIMENTAL PROCEDURES

Chemicals. Only high-purity reagents were used. Molecular biology-grade Tris base, β-mercaptoethanol and dithiothreitol (all certified RNase and DNase free by the manufacturer), bovine serum albumin, fraction V, and diethylpyrocarbonate were from Sigma (St. Louis, MO), aqueous 1 M triethylammonium acetate was from Fluka BioChemika (Buchs, Switzerland), tetrabutylammonium fluoride solution, 1 M in tetrahydrofuran, was from Aldrich Chemical Company (Milwaukee, WI), RNA phosphoramidite monomers were from Glen Research (Sterling, VA), HPLC-purified GMP−PNP was from ICN (Irvine, CA), ultrapure GTP was from Pharmacia (Uppsala, Sweden), Bio-Rad protein assay dye reagent and Bio-Gel P-2, extra fine, were from Bio-Rad Laboratories (Richmond, CA), translation-grade [^{35}S]methionine was from NEN (Boston, MA), the SurePure TLC kit used for oligonucleotide purification was from United States Biochemical (Cleveland, OH), and the plastic-supported silica gel 60 f_{254} precoated TLC plates were from EM Reagents (Darmstadt, Germany). All other materials were at least reagent grade: acetonitrile, ammonium hydroxide, mono- and dibasic sodium phosphate, ethanol, glycerol, KCl, magnesium acetate, and toluene.

Buffers. Buffer A: 50 mM Tris·HCl, pH 7.8, 5 mM β-mercaptoethanol, 100 μM EDTA, and 10% glycerol; buffer B: 20 mM Tris·HCl, pH 7.8, 100 mM KCl, 1 mM magnesium acetate, 5 mM β-mercaptoethanol, and 10% (v/v) glycerol; buffer C: 20 mM Tris·HCl, pH 7.8, 100 mM KCl, and 1 mM magnesium acetate.

Instrumentation and Data Analysis. Fluorescence anisotropy measurements were made using the method of Giblin (1978), a modification of the DeSa and Wampler method (1973) with modulation of the exciting light. The fluorimeter (Alphascan, Photon Technology, Inc.) was used with a Lexel (Palo Alto, CA) Model 75 argon ion laser with 488-nm light as the excitation light source, and data were collected using PTI's Alphascan software. A Model 01 01 PEM 80 Hinds International, Inc. (Portland, OR) photoelastic modulator was positioned between the laser and the cuvette to modulate the excitation light. For each emission anisotropy measurement, 100 data points were collected in 1 s at 518 nm for unmodulated excitation, followed immediately by collection of 100 data points for modulated excitation (PEM 80 retardation = 595.4 nm). Each set of points was fit by linear regression analysis; the last point of the fitted line was recorded as the emission intensity for the unmodulated reading, and the first point of the fitted line was used for the second, modulated case. The very slight effect of photobleaching of the fluorescein by the exciting light was thus essentially eliminated. The cuvette compartment was thermostated at 15 °C using a Lauda (Model K-2/R) constant temperature circulating water bath for all anisotropy measurements. Measurements were taken at 3−5-min intervals after the components were mixed and thermally equilibrated, until three consecutive measurements yielded a value ±0.005 from the previous measurement, and the values were averaged. Typically, three to five measurements were required. The small contribution to the emission anisotropy, $\langle r \rangle$, from scattering of the incident 488-nm laser line was nearly eliminated by positioning a long pass filter between the cuvette and the emission detector. In all instances, the small residual light scattering contribution to $\langle r \rangle$ was corrected for by subtracting the fractional contribution due to scattering from the observed $\langle r \rangle$.

A standard filtration system using 25 mm diameter/0.45 μm pore type HA filters and vacuum/pressure pump from Millipore (Bedford, MA) were used for assays. Samples were measured for radioactivity in 7 mL of toluene containing 0.04% (w/v) Omnifluor from DuPont (Boston, MA) in a Packard (Downers Grove, IL) 1600TR liquid scintillation counter.

Preparation of Initiation Factors, Ribosomes, and Message. CM−Sephadex-purified eIF-2 was obtained using the method of Das et al. (1982). This eIF-2 preparation contained the 67-kDa polypeptide in addition to the three subunits of eIF-2 in approximately a 1:1 mole ratio. Active three-subunit eIF-2 was isolated from this material as follows: The protein solution, typically 3−5 mg, was dialyzed against buffer A containing 100 mM KCl. The dialyzed protein (2−5 mL) was clarified by centrifugation at 10000*g* for 10 min at 4 °C, injected at a flow rate of 1 mL/min onto a Mono-S HR 5/5 cation-exchange column equilibrated with 50 mL of buffer A containing 100 mM KCl, washed with 10 mL of the same buffer, and eluted with a linear salt gradient of 100−400 mM KCl in buffer A over 30 mL. The 67-kDa polypeptide and the purified three-subunit eIF-2 eluted at approximately 175 mM KCl and 325 mM KCl, respectively. The fractions were analyzed for purity using 15% SDS−PAGE and Coomassie blue stain, and the peak fractions were stored in liquid nitrogen. Purified Co-eIF-2C was obtained following the method of Roy et al. (1988) without modification. Non-radiolabeled Met-tRNA$_f^{Met}$ and [^{35}S]Met-tRNA$_f^{Met}$ were prepared identically, following the procedure of Gupta et al. (1973). The extent of charging for the [^{35}S]Met-tRNA$_f^{Met}$ was calculated from the specific activity of the incorporated [^{35}S]methionine; we assumed the same level of charging for the non-radiolabeled Met-tRNA$_f^{Met}$. The preparation of 40S ribosomal subunits from rabbit reticulocyte lysate has been previously described (Woodley et al., 1974). The concentrations of rabbit reticulocyte 40S ribosomal subunits were determined by absorption spectroscopy using 1 A_{260} unit =

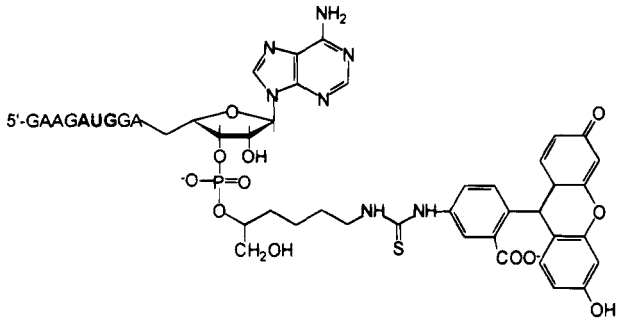

FIGURE 1: Structure of the 3′-end fluorescein-labeled RNA 10-mer.

50 pmol of 40S, reported for human placental 40S ribosomal subunits (Matasova et al., 1991).

The 5′-AUG-3′ RNA trinucleotide was purchased from Synthetic Genetics (San Diego, CA) and used without further purification. Both of the AUG-containing 10-mer oligoribonucleotides, 5′-GAAGAUGGAA-3′ and 5′-GAAGAUGGAA-3′-*F (the same 10-mer labeled at the 3′-end with fluorescein), were purchased from Research Genetics (Huntsville, AL); these 10-mers required further purification, described below. The five RNA 10-mers containing various mutations in the AUG codon were synthesized by our departmental oligonucleotide synthesis facility, and their preparations were completed as described below. Throughout these procedures, extreme care was taken to avoid the introduction of RNases into the samples, including sterilization and DEPC treatment of materials wherever possible.

Purification of 5′-GAAGAUGGAA-3′. Preliminary TLC results showed polynucleotides of multiple lengths in the commercial preparation. (TLC was done using plastic-supported silica gel 60 f_{254} precoated plates, developed with 80% v/v acetonitrile in water.) To isolate RNA decamers, the preparation was purified using a SurePure TLC kit following the protocol supplied with the kit. The 10-mer RNA band was removed and eluted from the silica into sterile DEPC-treated water. To check that the strongly basic (pH > 13) mobile phase used in the TLC procedure had not hydrolyzed the 10-mer, an aliquot of the purified oligomer was re-run on a fresh plate, where it migrated as a single spot with the same R_f value as in the first run. Of the initial A_{260} units, 8% migrated as a 10-mer, and that material was recovered and used immediately.

*Purification of 5′-GAAGAUGGAA-3′-*F.* The structure of the oligomer showing the linkage of fluorescein is given in Figure 1. Preliminary TLC results showed that approximately 90% of the total fluorescence in the commercial preparations derived from free fluorescein. The labeled oligomer was separated from the free fluorescein on a Bio-Gel P-2 column, eluting with 0.01 M sodium phosphate buffer, pH 7.2. The labeled RNA migrated as a faster, narrow band, and was shown by TLC and absorbance spectroscopy to comprise 11% of the total initial sample. The free fluorescein was clearly separated in a broad trailing band. The extinction coefficients used throughout were as follows: RNA, pH 7.2, $\epsilon_{260\ nm}$ (per 10-mer), 100 $mM^{-1}\ cm^{-1}$ (Research Genetics product data sheet), and fluorescein, pH 7.2, $\epsilon_{492\ nm}$, 70 $mM^{-1}\ cm^{-1}$ and $\epsilon_{260\ nm}$, 25 $mM^{-1}\ cm^{-1}$. The extinction coefficients for fluorescein were based on an $\epsilon_{492\ nm}$ of 75 $mM^{-1}\ cm^{-1}$ in 20 mM Tris·HCl, pH 9.0 (Haugland, 1992).

Preparation of RNA Oligomers with Modifications in AUG. The following 10-mer oligoribonucleotides with various alterations in the AUG sequence (shown underlined) were prepared using a 0.2-μmol scale synthesis with RNA phosphoramidite monomers: (1) 5′-GAAGGUGGAA-3′, (2) 5′-GAAGAUAGAA-3′, (3) 5′-GAAGAGGGAA-3′, (4) 5′-GAAGGCGGAA-3′, (5) 5′-GAAGUUGGAA-3′. Following synthesis, each oligomer was cleaved from its column and deprotected using a modification of the protocol described in the Glen Research Corp. (Sterling, VA) Technical Bulletin *Deprotection of Synthetic Oligoribonucleotides.* Cleavage from the solid support was accomplished by first aspirating 0.5 mL of ethanolic ammonium hydroxide (1 vol of ethanol:3 vol of ammonium hydroxide, specific gravity 0.88) into the synthesis column using a 10-mL syringe. After 1 h at room temperature, the solution was ejected from the column into a 5-mL glass vial. This process was repeated three additional times. The column was then opened, and the support was rinsed into the vial with 0.5 mL of ethanolic ammonium hydroxide. The vial was sealed and stored at 55 °C for 17 h to cleave any residual 10-mer from the support matrix and then briefly chilled on ice. The supernatant was removed and evaporated to dryness by vacuum centrifugation. The 2′-silyl protecting groups were removed by adding 0.4 mL of a 1 M tetrabutylammonium fluoride solution in THF to the dried residue. The suspensions were vortexed vigorously and stored at room temperature for 14 h; 0.4 mL of 1 M aqueous TEAA, pH 7, was then added. The oligomers were desalted on a 10-mL Bio-Gel P-2 column; they were eluted, using DEPC-treated sterile water, in the void volume, with absorbance monitored at 260 nm. The peak fractions were evaporated to dryness, pooled, and resuspended in approximately 300 μL of DEPC-treated water. A SurePure TLC analysis of each oligomer showed that in each case the 10-mer band contained at least 95% of the total material. The oligomers were used immediately and without further purification.

Spectroscopic Measurements. Determination of K_a(R,M). Purified 40S ribosomal subunits (6 μM) were titrated into 250 μL of an 8 nM solution of 5′-GAAGAUGGAA-3′-*F in buffer B. Anisotropy measurements were recorded after each addition (1−10 μL) of R, and an average value of $\langle r \rangle$ was obtained for each of the 10 additions as described above. The final concentration of R ranged from 0 to 1060 nM. The optimal values for K_a(R,M) and r_{max} were determined using a Simplex algorithm (Noggle, 1985) to minimize the sum of squared residuals, $\sum(\langle r \rangle_{obs} - \langle r \rangle_{calc})_i^2$, where

$$\langle r \rangle_{calc_i} = \frac{r_{max}(R{\cdot}M{*}F)_i + r_o(M{*}F_{free})_i}{M{*}F_{total_i}} \quad (1)$$

and i indexes the 10 additions of R, r_{max} is the anisotropy of the R·M*F complex, and r_o is the anisotropy of M*F; $(R{\cdot}M{*}F)_i$ and $(M{*}F_{free})_i$ derive from K_a(R,M), $M{*}F_{total,i}$, and $R_{total,i}$. This analysis assumes single-site binding of M to R. Error estimates for K_a(R,M) and r_{max} were obtained from the variance matrix.

Determination of K_a(Q,M). The concentrations of eIF-2 and Co-eIF-2C were determined using a Bio-Rad protein assay with BSA as the standard and values for M_r(eIF-2) of 144 000 and M_r(CO-eIF-2C) of 600 000. The use of the nonhydrolyzable GTP analogue, GMP−PNP, has been

reported to stabilize the ternary complex (Roy et al., 1984) and was used in lieu of GTP for the spectroscopic assays. To form Q, a 250-μL solution containing 100 μM GMP–PNP, 0.960 μM eIF-2, 2.9 μM Co-eIF-2C, and 1.9 μM Met-tRNA$_f^{Met}$ in buffer B was incubated at 37 °C for 5 min (conditions previously determined to be optimal). The preparation of Q was used immediately in the spectroscopic studies. Because the formation of Q is not 100% efficient, the concentration of the complex was determined by preparing Q precisely as described above, except [^{35}S]Met-tRNA$_f^{Met}$ (15 000 cpm/pmol) was substituted for Met-tRNA$_f^{Met}$. Following the incubation, the solution was subjected to Millipore filtration, which traps the Q complex but not free tRNA. The radioactivity from retained [^{35}S]Met-tRNA$_f^{Met}$ therefore corresponded to the concentration of Q formed. A control assay was done, omitting eIF-2, and the sample counts corrected accordingly. Both assays were done in triplicate, the counts were averaged, and the specific activity of the [^{35}S]Met-tRNA$_f^{Met}$ was used to convert the counts to concentration. We assumed the same concentration of Q was formed when unlabeled tRNA was used.

The extent to which the fluorescein-labeled RNA (M*F) bound to each of the components that comprise Q was determined first. The anisotropy of 8 nM M*F was measured in buffer B at 15 °C. In separate experiments, M*F was added to a final concentration of 8 nM to 250 μL solutions of 1.07 μM Co-eIF-2C, 0.4 μM Met-tRNA$_f^{Met}$, and 0.655 μM eIF-2 in the same buffer at 15 °C, and the anisotropy was measured. There was no measurable change in the anisotropy to within the error of the measurements with any of these components, and we concluded that, in the concentration range of our experimental work, binding of the 10-mer RNA to those three components was negligible. Preliminary titration of Q into M*F likewise had shown no change in the measured anisotropy of the M*F. To maintain a high concentration of Q, a single addition of M*F was added to a final concentration of 8 nM to 250 μL of 0.595 μM Q, and six measurements of anisotropy were made. The average of these measurements was within the error of the anisotropy measured for RNA alone, and our conclusion was that binding between Q and M was absent or negligible. In order to establish an absolute upper limit on binding between the two, we assumed that the slight increase in the average $\langle r \rangle$ resulted from binding and was *not* negligible. We then assigned a value to r_{max} equal to the value that we had obtained for R•M*F, assuming that this would be an upper limit. From this single measurement, an estimate of K_a(Q,M) was determined using the relationship

$$\langle r \rangle = \frac{r_{max}(\text{Q•M*F}) + r_o(\text{M*F}_{free})}{(\text{M*F}_{total})} \quad (2)$$

where $\langle r \rangle$ is the observed anisotropy, r_{max} is the anisotropy of the Q•M*F complex, r_o is the anisotropy of M*F, and Q•M*F is written in terms of (M*F$_{total}$), (Q$_{total}$), and K_a(Q,M).

Millipore Filtration Assays. Millipore filtration has been used extensively to assay the binding of Q to R. The assays rely on two facts: (1) the nitrocellulose-based filters specifically trap protein and ribosomal complexes but allow free Met-tRNA$_f^{Met}$ to pass through the membrane and (2) in the presence of 5 mM Mg^{2+}, *free* Q dissociates (over 40 min) into its four components (Roy et al., 1988), which include initiator tRNA. Q is therefore prepared using radiolabeled [^{35}S]Met-tRNA$_f^{Met}$ and incubated with either R or R + M to form the respective binary ([^{35}S]Q•R) or ternary ([^{35}S]Q•R•M) complexes. Mg^{2+} is then added to 5 mM, causing dissociation of all free [^{35}S]Q (Q not in Q•R or Q•R•M complexes). The sample solution is subjected to filtration; the [^{35}S]Met-tRNA$_f^{Met}$ released from the uncomplexed Q passes through the filter, and the [^{35}S]Q•R and [^{35}S]Q•R•M complexes are trapped. The counts on the filter (after background corrections) therefore correspond to the total concentration of complex formed. This assay was used to obtain K_a(Q,R) and K_a(Q,R•M).

For the filtration assays, Q was made using GTP rather than GMP–PNP, since our method of analysis required GTP, and the complex was stable during the time needed to complete the assays. Background counts derived from two sources: nonspecific binding of [^{35}S]Met-tRNA$_f^{Met}$ to reaction components other than eIF-2 and a slight GTP-independent binding. GTP is required for Met-tRNA$_f^{Met}$ binding too eIF-2 to form Q, and in the absence of GTP, no counts should be retained on the filter. In practice, a slight GTP-independent background count was measured. Replicate control assays were therefore conducted, omitting eIF-2 and GTP, respectively, and these background counts were subtracted at each time point from all experimental data. The specific activity of the [^{35}S]Met-tRNA$_f^{Met}$ was calculated in the standard way (Woodley et al., 1974) and was used to convert counts to concentration. Because we wanted precise data from which to calculate equilibrium constants, it was important to understand what was occurring at each step of the assay and to determine the kinetics of the various association and dissociation reactions that occurred during the incubations, with particular attention to potential shifts in equilibria. In order to combine the thermodynamic values obtained from the spectroscopic and filtration studies, the assays were done with incubations at 15 °C, the temperature at which all spectroscopic measurements were made, rather than the usual 37 °C.

(A) Assay Reaction Kinetics. Kinetics of Q, Q•R, and Q•R•M Formation at 15 °C. To form Q, 75-μL solutions were made containing the following: 20 mM Tris•HCl, pH 7.8, 100 mM KCl, 1 mM magnesium acetate, 2 mM DTT, 10 μg of BSA, 0.267 mM GTP, 92 nM eIF-2, 0.53 μM Co-eIF-2C, and 0.15 μM [^{35}S]Met-tRNA$_f^{Met}$ (10 000 cpm/pmol). The solutions were incubated at 15 °C for 0, 5, 10, 20, 40, and 60 min with the binding reaction terminated by the addition of 3 mL of ice cold wash buffer C. The reaction mixtures were filtered; the filters were washed with 6 mL of buffer C, baked at 130 °C for 5 min, and counted for radioactivity. At each time point, the concentration of Q was taken to be equivalent to the concentration of [^{35}S]Met-tRNA$_f^{Met}$, assuming one tRNA per complex and that filtration trapped 100% of the complex. The maximum amount of Q (49.7 nM) was formed in $t \leq 5$ min and remained stable for at least 60 min. The kinetics of the formation of Q•R complex and Q•R•M complex at 15 °C were determined using the assay outlined previously: In stage I, Q was formed exactly as described above, using an incubation time of 20 min. In stage II, 0.2 A_{260} unit (10.2 pmol, 136 nM) 40S ribosomal subunits were added, either with or without 27 μM AUG triplets, and the solutions were incubated at 15 °C for 0, 5, 10, 20, 40 and 60 min. In stage III, dissociation of Met-tRNA$_f^{Met}$ from Q *not* bound to R was accomplished by adding magnesium acetate to a final concentration of 5

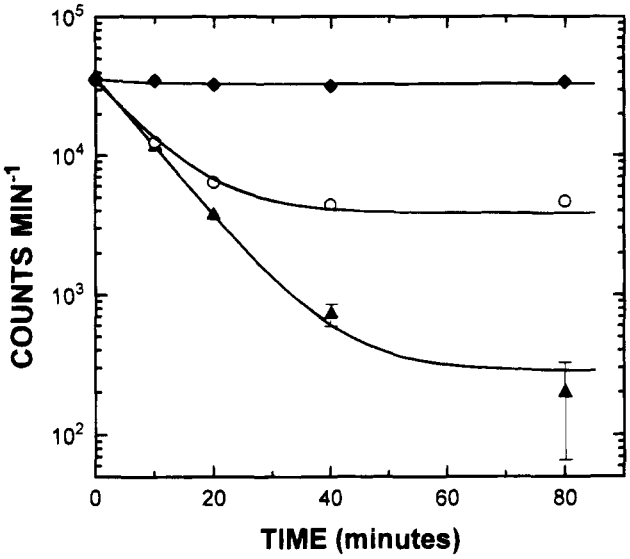

FIGURE 2: Kinetics of the Mg^{2+}-induced dissociation of Met-$tRNA_f^{Met}$ from Q in solutions of Q, Q + R, and Q + R + M. Dissociation of Q for Q alone (triangles), for Q + R (open circles), and for Q + R + M (diamonds) was measured at the times indicated following the addition of 5 mM Mg^{2+}. The curves are from the optimal fit to eq 3 for Q data and eq 4 for both Q + R and Q + R + M data. Error bars exceeding the height of the marker are shown. The initial slope of the curve corresponding to Q alone has a $t_{1/2}$ of 5.9 min. At $t = 0$, the counts corresponding to Q = 37 282 cpm.

mM and storing on ice for 40 min. Millipore filtration was performed as described, with the counts corresponding to total complex, (Q·R) or (Q·R + Q·R·M). In practice, "0" time was approximately 1 min, taking into account the time required to manipulate the solutions, and the maximum concentration of both complexes was formed within this time. The assay was subsequently done with a 5-min incubation in stage II.

Kinetics of Mg^{2+}-Induced Met-$tRNA_f^{Met}$ Dissociation from Q. In order to define the end point of the assay, it was necessary to understand the time course of Met-$tRNA_f^{Met}$ dissociation from Q. The assay protocol assumed that 5 mM Mg^{2+} caused Met-$tRNA_f^{Met}$ to dissociate only from Q not bound to R and also that the equilibrium concentrations of Q·R and Q·R·M were not altered during this process. To determine the validity of these assumptions, Q was formed as described; magnesium acetate was added to 5 mM, and the solutions were stored on ice for varying times (0, 10, 20, 40 and 80 min) as indicated in Figure 2. These data, which gave the time course of Met-$tRNA_f^{Met}$ dissociation from Q alone, were analyzed as described below and subsequently used to understand the kinetics of Q dissociation in solutions containing Q and R and Q, R, and M.

The kinetic data for dissociation of Met-$tRNA_f^{Met}$ from isolated Q were very well fit by a model that assumed that first-order decay plus a small constant would describe the counts on the Millipore filters:

$$\text{counts}_{(t)} = \left(\frac{\text{counts}_{t=0}}{1+\varrho}\right)(\varrho e^{(-k_Q t)} + 1) \qquad (3)$$

where k_Q is the first-order rate constant and ϱ is the ratio (at long time) of the amount of Q that decays by first order to the amount of residual material. At $t = 0$, 37 282 cpm were measured, which corresponded to the initial 49.7 nM of Q. The optimal value for k_Q was determined to be 0.118 min^{-1} and for ϱ was 130. Figure 2, bottom curve, shows the data points and the theoretical curve from eq 3. Since the residual material was <1% of the total Q, it was immaterial whether this second component was described by very slow decay or by a constant. The time to dissociate half of the total Q was 5.9 min. After 40 min, only 1% of the free Q remained.

We now wanted to demonstrate that we could account for the time course of Q dissociation, following the addition of Mg^{2+}, in the (Q,R) solution in terms of our understanding of the time response of isolated Q. The assay was performed, adding only 40S subunits in stage II. In stage III, the solutions were stored on ice for 0, 10, 20, 40, and 80 min, as for Q alone. We assumed that the value determined for ϱ in eq 3 characterized unbound Q in all samples. If, following the addition of Mg^{2+} ($t = 0$ min), there was a constant amount of Q·R complex and free Q dissociated according to eq 3, the following expression would pertain:

$$\text{counts}_t = \left(\frac{\text{counts}_{t=0} - B}{1+\varrho}\right)(\varrho e^{(-k_Q t)} + 1) + B \qquad (4)$$

where ϱ and k_Q are known from eq 3, and B, corresponding to the Q·R complex, is the only fitted parameter. The middle curve in Figure 2 shows the data points and the theoretically predicted curve obtained from eq 4, with the optimal fitted value of B = 3599 cpm. The very high quality of the fit confirmed our assumption that dissociation of Q·R was negligible in 5 mM Mg^{2+} for times up to 80 min.

The assay was repeated exactly as for Q·R except 1.5 μM AUG triplets were also added in stage II. The top curve of Figure 2 shows the data points for the time course of the Met-$tRNA_f^{Met}$ dissociation from Q in the mixture of Q, R, and M. The line was obtained by fitting eq 4 for B, which here corresponds to Q·R plus Q·R·M. The optimal value for B was 33 274 cpm, and the fitted value at each time point was within 3% of the measured value. The excellent fit indicated that we could account for the time course of Q dissociation in this solution in terms of our understanding of the kinetics of isolated Q and validated our assumption that no detectable shift in the equilibria of the complexes occurred during the course of the incubation. Since Q dissociation was essentially complete in all cases for $t > 40$ min, a 40-min incubation in stage III was used in all subsequent assays.

To ensure that we fully understood the source of the counts on the filter paper, a final control experiment was done. Two identical mixtures of Q were made as described, with incubation at 15 °C for 20 min. To one of the mixtures, 10-mer RNA was added to a final concentration of 2.8 μM (approximately double the concentration used in the assays to determine the equilibrium constants). The solutions were made 5 mM in magnesium acetate and incubated on ice for 40 min, and the counts were recorded. This assay was performed two times and was also done using the optimal incubation conditions for Q formation, 37 °C for 5 min. In each case, the end points for the Q and Q + M solutions differed within our experimental error; the effect of M was thus insignificant. This result confirmed that B in eq 4 corresponded accurately to the total concentration of complex, Q·R plus Q·R·M.

(B) Determination of Equilibrium Association Constants. $K_a(Q,R)$. The three-stage assay described in (A) above was

used: In stage I, Q formation, six identical solutions were prepared; the conditions were identical to those in (A), and it was assumed that the same initial amount of Q was formed. In stage II, 40S ribosomal subunits were added in 1−10-μL additions to final concentrations of 0, 6.8, 20.4, 68, 204, and 612 nM, and the solutions were incubated for 5 min at 15 °C. In stage III, magnesium acetate was added to a final concentration of 5 mM, and the solutions were stored on ice for 40 min. Millipore filtration was performed, and the concentration of the Q·R complex formed at each concentration of R was determined from the counts.

The value of K_a(Q,R) was obtained from

$$\nu_i = \frac{K_{a(Q,R)}R_i}{1 + K_{a(Q,R)}R_i} \quad (5)$$

where i indexes the additions of R, ν is the fraction of bound Q, and R is the concentration of free 40S ribosomal subunits. Total Q and R were known. To re-confirm the validity of eq 4, that equation was solved for B at $t = 40$ min for each addition of R, using the values previously determined for ϱ and k_Q. The value calculated for B (corresponding to the concentration of Q·R complex) at each point was within 1.7% of the measured counts. The fitted values of B were converted to concentration and used to obtain ν and (free R) in eq 5. The error in K_a was determined from the variance matrix.

K_a(Q·R,M). To obtain the binding data for K_a(Q·R,M), a second set of assays was performed concurrently with the assays described above for K_a(Q,R). The procedure described was followed exactly except 1.5 μM 10-mer RNA (final concentration) was added in stage II to each solution in addition to 40S ribosomal subunits.

The value for K_a(Q·R,M) was determined as follows. Three conservation equations were written for *total* Q, R, and M (all known) in terms of the concentrations of free Q, R, and M and the various equilibrium constants. The values for all equilibrium constants were now known except that for K_a(Q·R,M), which was the only fitted parameter. As K_a(Q·R,M) was varied, a three-dimensional Newton−Raphson procedure, with variable step-size, was used to solve the three nonlinear conservation equations for free Q, R, and M for each addition of R and M; the value of total bound Q, (Q·R) + (Q·R·M), was then calculated directly. The observed value of (Q·R) + (Q·R·M) was from the counts measured at each point. K_a(Q·R,M) was varied to minimize the sum of squared residuals for observed vs calculated (Q·R) + (Q·R·M). It is immaterial whether one fits for K_a(Q·R,M) or K_a(Q,R·M), owing to the thermodynamic cycle shown in Figure 5, since

$$[K_a(Q,R)][K_a(Q{\cdot}R,M)] = [K_a(R,M)][K_a(Q,R{\cdot}M)] \quad (6)$$

An estimate of the error in K_a(Q·R,M) was obtained as follows. All possible combinations of $K_a \pm \sigma_K$ were taken for the binary association constants, and the maximum variation in K_a(Q·R,M) was determined as that value that intersected the 68% confidence contour of the F-statistic. This procedure gave a larger error estimate than would have been obtained for the variation of K_a(Q·R,M) alone.

Multiple-Site Binding of M to R. It may be that multiple nucleotide binding sites around the AUG codon are present on the 40S subunit; since our mRNA analogue was a short oligonucleotide, more complex models for the binding of M were also considered. Multiple binding of the 10-mer M to an extended nucleotide binding site on R is an example of a multivalent ligand binding to a lattice (McGhee & von Hippel, 1974): Let Y_M be the mole fraction of ligand (M) that is bound to the ribosome, and R_T and M_T be the total concentration of 40S and M, respectively. If $\langle\nu\rangle$ is the average number of bound ligands per ribosome, then

$$Y_M = (R_T/M_T)\langle\nu\rangle = (R_T/M_T)(\partial \log D/\partial \log M) \quad (7)$$

where D is the binding polynomial for M binding to R and is in terms of free M and K_M, the constant for the multivalent M binding to a single site on the ribosome. We assume that only one K_M characterizes the binding and postulate a 30-site region on R for nucleotide binding in keeping with the initiator region in prokaryotes. If end effects in the binding are neglected, that is, all 10 bases are required to be bound to R whenever the 10-mer M is bound, then there are 21 ways for binding a single M to a ribosome having 30 sites for base binding, 66 ways to accommodate two M's, and only one way to bind three M's. The binding polynomial is then as follows: $D = 1 + 21K_MM + 66(K_MM)^2 + (K_MM)^3$. The negative reciprocals of the zeroes of D are the three apparent binding constants for binding one, two, and three M's at three distinct sites, and these will be in the ratios: 1:0.223:0.00089, giving the appearance of heterogeneity or anti-cooperativity in the binding of M to R provided $\langle\nu\rangle$ is sufficiently large in the experiment. The data for M binding to R were analyzed according to this simple lattice model as follows: Free M was written as $M_T(1 - Y_M)$, and $\Sigma(Y_M^{observed} - Y_M^{calculated})^2$ was minimized by varying the parameter K_M. $Y_M^{calculated}$ was obtained from the right side of eq 7 using $M_T(1 - Y_M^{observed})$ for M.

Binding of *both* Q and M to R was also analyzed in terms of the lattice model. Let the binding polynomial above be denoted as $1 + P$, where P is the polynomial in terms of K_MM for the first through third powers. If K_Q and K_{QE} are the association constants for the binding of Q to R with and without bound M, respectively, then the binding polynomial for the simplest lattice model (case 1) is $D = 1 + K_Q(Q) + P + PK_{QE}(Q)$. Alternatively, the Q·R·M complex can be formed by Q and R binding initially, followed by M binding; in this view, prior binding of Q may potentially enhance the binding of M. If K_M and K_{ME} are the binding constants for M binding to R without and with bound Q, respectively, the binding polynomial is $D = 1 + K_Q(Q) + P + P'K_Q(Q)$, where P' is simply P with K_M replaced by K_{ME} (case 2). These two mathematical models assume that prior binding of Q affects all binding sites for M equally or that binding of each M to any of the sites on R will enhance the binding of Q by the same amount. A final simple model (case 3) in accord with biochemical evidence considers that Q binds to a distinct site on R and that enhancement of binding of M occurs only when there is proper alignment of the AUG codon, implying that only one microstate of the Q·R·M complex is formed with enhancement of binding; for all other microstates, binding of Q and M are independent. In this case, there are 20 ways of binding one M without enhancement of Q binding; 55 ways of binding two M's without enhancement and 11 with enhancement; and only one way of binding all three M's. The binding polynomial is $1 + K_Q(Q) + P + K_{QE}K_M(M)(Q) + 20\ K_MK_Q(M)(Q) + 11K_{QE}K_M^2(M)^2(Q) + 55K_QK_M^2(M)^2(Q) + K_{QE}K_M^3(M)^3(Q)$.

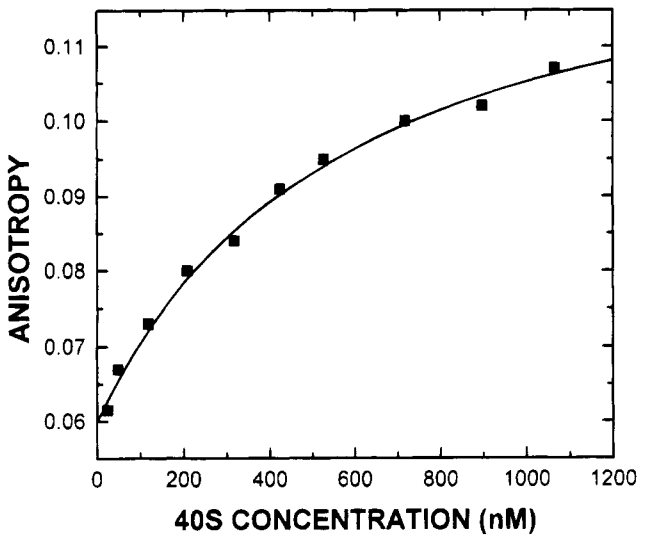

FIGURE 3: Titration of 5′-GAAGAUGGAA-*F-3′ (M) with 40S ribosomal subunits (R). Small volume additions (1−10 μL) of a 6.0 μM solution of R were made into an 8 nM solution of M (initial volume, 250 μL), and the anisotropy was measured after each addition.

Data for the binding of Q to R in the presence of M were analyzed according to these lattice models (cases 1−3) using an extended Newton−Raphson routine.

(C) Dependence of the Formation of Q·R·M on the Sequence of M. We investigated the effect of AUG-modified M on the binding of Q to R using Millipore filtration assays as described above for K_a(Q·R,M), substituting each of the five modified RNA 10-mers for the AUG-containing oligomer. Because our intent was to obtain only this single piece of binding information for the modified RNA 10-mers, and not to undertake a complete investigation of the thermodynamic values that characterize the formation of Q·R·M_{nonAUG}, the assays were done using the conditions known to optimize Q formation. The modifications in the assays as described in (B) were as follows: For Q formation in stage I, incubation was at 37 °C for 5 min. In stage II, which results in Q·R·M formation, the final concentration of 40S was 72 nM (0.108 A_{260} unit, 5.4 pmol). The final concentration of AUG triplet was 27 μM and of all RNA 10-mers, 8.2 μM (0.05 A_{260} unit for triplet and 10-mers), and the incubation was for 2 min at 37 °C.

RESULTS

K_a(R,M). As shown in Figure 3, each addition of 40S into M*F resulted in an increased anisotropy. The two parameter fit, varying K_a(R,M) and r_{max}, gave an excellent fit to the data, with a K_a(R,M) of 1.78 ± 0.21 × 10^6 M^{-1} and an r_{max} of 0.131 ± 0.004.

K_a(Q,M). The measured anisotropy of M*F was 0.079 ± 0.005. When M*F was added to 0.595 μM Q, the measured anisotropy was 0.083 ± 0.007, indicating either no binding or a low affinity of Q for M*F. To obtain an upper limit for K_a(Q,M), we assumed that the small increase in ⟨r⟩ for Q + M was *not* negligible and, from the single value for ⟨r⟩, used eq 2 to calculate a value for K_a(Q,M) of 0.14 × 10^6 M^{-1}. Were there *no* local motion of the probe, r_{max} would be greater than 0.39 for both the Q·M*F complex and the R·M*F complex, for Q and R modeled as spheres. The fitted value for r_{max} of 0.131 determined previously for the R·M*F complex is consistent with the fluorophore moving within a cone half-angle of approximately 55°, characteristic of considerable local motion (Bucci & Steiner, 1988). We assumed the local motion of the fluorophore would be similar for M*F binding to Q and so assigned to r_{max} in eq 2 a value of 0.131. We therefore estimated that K_a(Q,M) was between 0 and 0.14 × 10^6 M^{-1}.

Table 1: Binding Constants and Corresponding Free Energy Changes Calculated for Interactions of Q (Quaternary Complex, eIF-2·GTP·Met-tRNA$_f^{Met}$·Co-eIF-2C), R (40S Ribosomal Subunit), and M (a Synthetic RNA 10-mer Containing Initiation Codon 5′-GAAGAUGGAA-3′)[a]

inter-action	K_d × 10^9 (M)	K_a × 10^{-6} (M^{-1})	$\Delta G°$ (kcal/mol)
Q,R	1060	0.94 (± 0.05)	−7.87 (−7.84 to −7.90)
R,M	560	1.78 (± 0.21)	−8.24 (−8.16 to −8.30)
Q,M	+ ∞	0	+ ∞
	[7143]	[0.14]	[−6.78]
Q·R,M	9.1	110	−10.60
	[7.5]	[133 (95−194)]	[−10.71 (−10.51 to −10.93)]
Q,R·M	17.2	58.2	−10.23
	[14.2]	[70.2 (50.2−102)]	[−10.34 (−10.15 to −10.56)]

[a] The errors for each constant are in parentheses. The values in brackets were obtained with K_a(Q,M) = 0.14 × 10^6 M^{-1}. $\Delta G°$ was calculated for the association reaction and a standard state of 1 M.

K_a(Q,R) and K_a(Q,R·M). Control experiments were done as described previously with each assay, and the data were used to correct the experimental data points. The background counts obtained throughout the study were quite constant with a mean value of 1496 cpm and the standard error of the mean of 122 cpm.

The Q + R assays were done with total Q constant at 49.7 nM. The 40S concentrations used were 6.8, 20.4, 68, 204, and 612 nM. The respective concentrations of Q·R complex formed were as follows, with the measured cpm given in parentheses: 1.04 nM (784 cpm), 1.60 nM (1200 cpm), 3.27 nM (2454 cpm), 7.70 nM (5775 cpm), and 7.12 nM (5343 cpm). The fraction of Q bound (ν in eq 5) at each 40S addition was (Q·R)/Q_{total}; free R was simply total R at each point minus (Q·R). The value of K_a(Q,R) calculated from these data using eq 5 was 0.94 ± 0.05 × 10^6 M^{-1}.

In the Q + R + M assays, total Q and total 10-mer RNA were constant at 49.7 nM and 1.5 μM, respectively. The retained counts corresponded to bound Q (Q·R + Q·R·M). The 40S concentrations were again 6.8, 20.4, 68, 204, and 612 nM; the respective concentrations of total complex formed, with observed cpm given in parentheses, were as follows: 3.61 nM (2709 cpm), 15.3 nM (11 502 cpm), 30.7 nM (23 006 cpm), 42.4 nM (31 821 cpm), and 45.3 nM (33 969 cpm). The fraction of bound Q was (Q·R + Q·R·M)/Q_{total}. These values (total R, M, and Q and the fraction of Q bound) together with the values of K_a(Q,R), K_a(Q,M) and K_a(R,M) (Table 1) were used in the fitting program to obtain the value for K_a(Q·R,M). The value of free R (R_{total} − (R·M) − (Q·R) − (Q·R·M)) at each point was calculated directly using the optimal value obtained for K_a(Q·R,M).

The value for K_a(Q·R,M) was determined using two different values for K_a(Q,M), due to the uncertainty in that association constant. When K_a(Q,M) was fixed at 0, the best fitting value for K_a(Q·R,M) was 110 × 10^6 M^{-1}; the value calculated from eq 6 for K_a(Q,R·M) was 58.2 × 10^6 M^{-1}. Then, K_a(Q,R·M)/K_a(Q,R) = 62; that is, Q bound to R·M

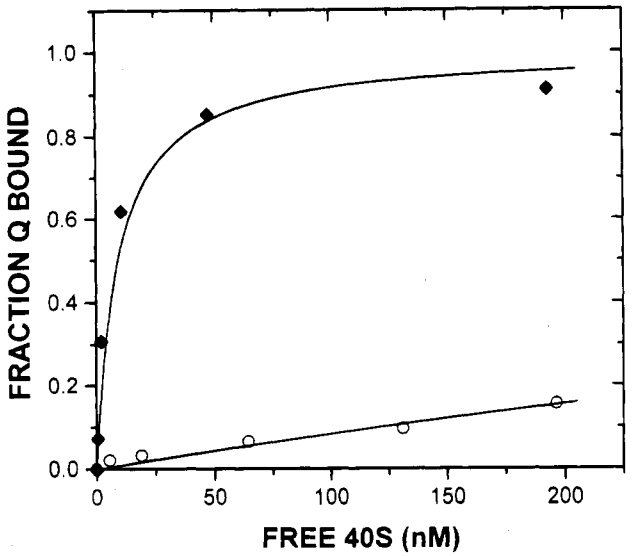

FIGURE 4: Titration of Q, and Q,M with R. The titrations of Q with R (open circles) and Q + 1.5 μM 5′-GAAGAUGGAA-3′ with R (diamonds) are shown. The Q + R data point at R_{free} = 130 nM is an independent measurement from the kinetic plot for Q + R in Figure 3 and is the fitted value of B in eq 4 at t = 40 min. The curves are from the calculated values for K_a(Q,R) and K_a(Q•R,M).

with 62× greater affinity than to R. When K_a(Q,M) was fixed at 0.14 × 10^6 M^{-1} (the estimated maximum value), the fitted value for K_a(Q•R,M) was 133 × 10^6 M^{-1}, and the sum of squared residuals was slightly greater than that obtained with K_a(Q,M) = 0. In this case, the value for K_a(Q,R•M) was 70.2 × 10^6 M^{-1}; the binding of Q to R was 75× greater with M previously bound. As one assigns to K_a(Q,M) increasingly larger values, the values for K_a(Q•R,M) and K_a(Q,R•M) also increase, resulting in larger enhancement factors. Therefore, setting K_a(Q,M) = 0 leads to a lower limit for ternary enhancement. Figure 4 shows the corrected data points for the Q,R titration and the Q,R•M titration with the analytically fitted curves.

Multiple-Site Binding of M to R. The binding of M to R was also analyzed according to the lattice model. Because most of the ribosomes were uncomplexed with M in these experiments ($\langle\nu\rangle$ was always less than 0.08), the heterogeneity implicit in a lattice model was scarcely evident. The sum of squared residuals at the minimum was 3.3× worse than for the simple single-site model (eq 1), but could not be rejected. As expected, the best fitting K_a, 0.0831 M^{-1}, was very nearly 21-fold less than for the single-site model, for which K_a was 1.78 M^{-1}, reflecting the predominant effect of the single occupancy of M on R and the effect of the statistical factor 21 in the lattice model.

For Q and M binding cooperatively to R, analysis according to case 1 gave K_{QE}/K_Q = 60, essentially the *same* enhancement as that for the single-site model. For case 2, the analysis is more complicated. The overall complex formation must be the same as for case 1; now, however, powers of K_{ME} appear that must have the same effect as the linear term K_{QE} in case 1. The optimum fit gave K_{ME}/K_M = 13.6, an apparent lower enhancement than obtained with the single-site model. In case 3, enhancement occurs for only *one* microstate of Q•R•M, that with the AUG aligned with the anticodon of Met-tRNA$_f^{Met}$. Here, K_{QE}/K_Q was 693/0.94, a much larger enhancement than for the single-site model. In this model, the same enhancement pertains for binding Q to R•M with M properly positioned as for binding M to R•Q at the single site.

Table 2: AUG Codon Dependence of 40S Initiation Complex Formation[a]

RNA oligomer added	pmol of Q bound to R		
	−M	+M	+M/−M
AUG	0.23	1.13	4.9
GAAGAUGGAA	0.21	0.84	4.0
GAAGGUGGAA	0.24	0.24	1.0
GAAGAUAGAA	0.24	0.27	1.1
GAAGAGGGAA	0.20	0.18	0.9
GAAGGCGGAA	0.20	0.21	1.05
GAAGUUGGAA	0.21	0.22	1.05

[a] The total concentrations of Q and R were 57 and 72 nM, respectively. The total concentration of M was 27 μM for AUG triplets and 8.2 μM for 10-mers.

Dependence of the Formation of Q•R•M on the Sequence of M. Millipore filtration assays were performed using AUG triplets, the RNA 10-mer containing AUG, and five other RNA 10-mers having one or two mutations within the AUG codon. The assay results are summarized in Table 2. In the presence of either AUG triplets or 5′-GAAGAUGGAA-3′, 4.9- and 4-fold more complex was formed, respectively, than when no M was present. However, no significant increase in radioactivity retained on the filters was measured for *any* of the modified RNA sequences: 5′-GAAGGUGGAA-3′, 5′-GAAGAUAGAA-3′, 5′-GAAGAGGGAA-3′, 5′-GAAGGCGGAA-3′, 5′-GAAGUUGGAA-3′.

DISCUSSION

Since this was an equilibrium study, it was essential to know by what time various species had reached their equilibrium concentrations and that these concentrations remained unchanged during the analyses. Further, if equilibria were accounted for, but the formation of Q•R were very much slower than that of Q•R•M, the filter assay would merely reflect kinetic control of the reaction and not thermodynamic control. Consider the scheme below, which summarizes the reactions:

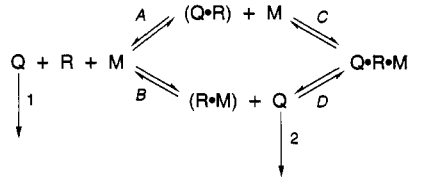

The scheme without paths 1 and 2 refers to the formation of binary complexes and Q•R•M; paths 1 and 2 refer to the irreversible dissociation of Q induced by Mg^{2+}. Our measurements indicate that the scheme is fully established in approximately 1 min; these are apparently fast reactions, with association processes occurring on the order of 10^6 M^{-1} s^{-1}. The 62-fold enhancement most likely derives from the difference in the rates of *dis*sociation of Q from Q•R and from Q•R•M. Having demonstrated that the Q•R and Q•R•M complexes were at equilibrium by the end of the stage II incubation and stable for at least 60 min, it was both necessary and sufficient for our thermodynamic analysis to show that (Q•R) and (Q•R•M) remained constant throughout the 40-min incubation following the addition of Mg^{2+}. The fact that we could account for the time course of Mg^{2+}-

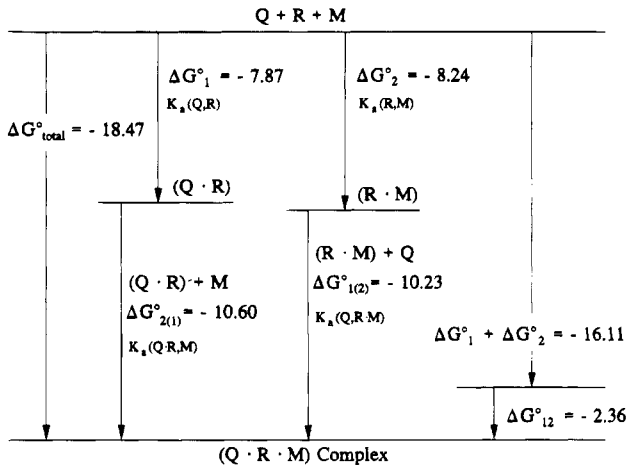

FIGURE 5: Weber free energy diagram for the ternary system involving Q, R, and M interactions. All interactions are drawn to scale, and units are in kcal mol^{-1} with a standard state of 1 M. At the top of the diagram, all components are present but unbound. The binary complexes Q·R and R·M and their energetics of formation are shown in the intermediate positions. A second decrease in free energy occurs when the third component binds to each binary complex, forming Q·R·M. Species 1 = Q and species 2 = M.

induced Q dissociation in the Q,R and Q,R,M solutions entirely in terms of our knowledge of the dissociation of Q alone (see Figure 2) rules out shifts in equilibria *A* and *D*, respectively. Shifts in equilibrium *C* are inconsequential, since our analysis measures only the sum Q·R + Q·R·M. Equilibrium *B* is also immaterial because all forms of Q not bound to R dissociate upon the addition of Mg^{2+} to 5 mM. From our combined kinetic analyses of the formation of these species and of the Mg^{2+}-induced dissociation of Q in solutions of Q, Q·R, and Q·R·M, we conclude that we have determined true equilibrium concentrations.

A summary of the binding constants and the calculated standard state free energy changes are in Table 1. The values of the free energy changes were used to create a free energy diagram (Figure 5) as proposed by Weber (1975). We define R as the macromolecule that binds ligands Q and M. By comparing the sum of the free energies of formation of Q·R and R·M with the observed free energy change for the overall reaction Q + R + M → Q·R·M, one can determine if positive or negative heterotropic interactions characterize the ligation to R. The difference between the standard state free energy change for formation of Q·R·M and the sum of the standard state ligation free energies for Q·R and R·M is the "coupling free energy" ($\Delta G°_{12}$) and is a direct measure of cooperativity (or anti-cooperativity). That is, $\Delta G°_{12} = \Delta G°_{total} - (\Delta G°_1 + \Delta G°_2)$. The coupling free energy for the Q + R + M ternary system is calculated to be −2.4 kcal/mol, indicative of high cooperativity.

As indicated in Figure 5, Q binds directly to the 40S ribosomal subunit with an association constant of 0.94×10^6 M^{-1}. The binding of Q to R is not, however, independent of message. $\Delta G°_1$ reflects the binding of species 1 (here, Q) to R; $\Delta G°_{1(2)}$ reflects the binding of species 1 to R already bound with species 2 (here, M). If the binding of Q to R were independent of M, the line corresponding to $\Delta G°_1$ would be equal in length to that for $\Delta G°_{1(2)}$. In fact, $\Delta G°_{1(2)} = \Delta G°_1 + \Delta G°_{12}$. That is, prior binding of M to R facilitates the binding of Q by 2.4 kcal/mol in terms of the standard state Gibbs free energy change or an increase by a factor of 62 in the association constant. The same $\Delta G°_{12}$ of interaction is obtained for the converse interaction ($\Delta G°_{2(1)} = \Delta G°_2 + \Delta G°_{12}$) so that prior binding of Q to R facilitates the subsequent binding of M, with the same free energy change and increase in K_a as above.

We report a range of values for the binding of M to Q and point out that as K_a(Q,M) increases, enhancement increases. Qualitatively, as more M is bound to Q in a binary complex, less M is responsible for the enhanced binding of Q to R observed experimentally. To compensate for the lower effective concentration of M, the binding of either M to R·Q or Q to R·M must be further enhanced. The simplest model for these interactions is provided by the single-site binding model on which Figure 4 is based. In the lattice models, however, the enhancement becomes model dependent and for essentially the same qualitative reason. In case 1, the enhancement for Q is the same as that for the single-site model, since it is merely a measure of how binding of M to R affects Q. In case 3, however, there are many ways of binding M to R that give no enhancement. In order to produce the observed cooperativity, there must be a large increase in K_{QE} over K_Q, 737, to compensate for these entropy effects. This enhancement corresponds to a $\Delta G°_{12}$ of −3.8 kcal/mol of Q, which, in the absence of more detailed information on the various nucleotide binding sites on the ribosome, may be taken as an upper limit for the cooperative interactions of R·Q with M containing AUG.

Goss et al. (1984) investigated cooperative interactions between the ternary system involving *E. coli* ribosomes, S1 ribosomal protein, and uridyl triplets and found a coupling free energy of −1.8 kcal/mol (in 6 mM Mg^{2+}). A coupling free energy of −2.4 kcal/mol is greater than any of those listed by Weber (1975) for diverse biochemical interactions. Clearly, the Q + R + M ternary system discussed here displays very high cooperativity.

The following perspective regarding initiation of protein synthesis is consistent with these data: Q and M bind to R with association constants that differ only by a factor of 2. When either Q or M binds to R, the highly cooperative nature of the ternary interaction makes binding of the other component much more probable, greatly increasing the efficiency of assembly of the 40S initiation complex. From our results, one could speculate that Q binds to the peptidyl site on the 40S ribosomal subunit, and the exposed AUG section of M binds to the same region of R, directly or by scanning. Either Q or M may bind first, with subsequent binding of the third component. This initial Q·R·M complex is formed with a free change that is simply $\Delta G°_1 + \Delta G°_2$. When the AUG codon in this initial Q·R·M complex is properly positioned, the complex is stabilized by a further decrease in free energy of 2.4 kcal/mol ($\Delta G°_{12}$), activating the complex for the next step of protein synthesis. In this view, it is immaterial whether M binds to the 40S ribosomal subunit directly at the initiation codon or scans to that position; once the AUG is in place, Q binds in a highly cooperative manner. Conversely, once Q binds, M binds with much higher affinity but only when the AUG region is properly aligned.

The difference measured in the energetics of the Q,R·M vs the Q,R interaction is in accord with the internal initiation model, but not with scanning models that assume the Q,R interaction to be independent of message. Our oligomer had no cap structure, and we included no eIF-4 group proteins

to facilitate binding; however, a short synthetic RNA may differ considerably in binding requirements from a native mRNA with complex secondary structure. The direct binding of M to R that we observed has not been observed in studies that use native mRNAs. In his review, Hershey (1991) points out that sucrose density gradient centrifugation may lead to erroneous conclusions when used to study equilibria, due to the very long analysis times required relative to the kinetic events occurring at the molecular level, and he suggests that may be the reason that stable complexes of R·M have not been observed.

Although no equilibrium constants were obtained for Q + M_{nonAUG}, R + M_{nonAUG} or Q·R + M_{nonAUG}, the Millipore filtration data from assays with M_{nonAUG} suggest that *only* AUG-containing message can enhance the binding of Q to R. The fact that we did not observe an increase in counts due to the presence of M_{nonAUG} may indicate no cooperativity (or even anti-cooperativity). That is, we do not have sufficient data at present to determine whether or not Q and M_{nonAUG} can be bound simultaneously on R. Perhaps, when the AUG sequence is not properly aligned with the ribosome and the factors comprising Q, no significant (or weaker) ternary Q·R·M interaction occurs. A simple simulation, using the count data in Table 2 and assuming the temperature dependence of the equilibrium constants to be negligible, showed enhancement to be essentially absent (<8%) for $0.18 \times 10^6\ M^{-1} < K_a(R,M_{nonAUG}) < 18 \times 10^6\ M^{-1}$. This result is consistent with Q and M_{nonAUG} binding independently and being positioned simultaneously on R, in accord with the model proposed above. Additional work to measure the equilibria for R·M_{nonAUG} and for the Q·R·M_{nonAUG} ternary complex is required for further understanding of this mechanism.

REFERENCES

Bucci, E., & Steiner, R. F. (1988) *Biophys. Chem. 30*, 199–224.

Darnbrough, C., Legon, S., Hunt, T., & Jackson, R. J. (1973) *J. Mol. Biol. 76*, 379–403.

Das, A., Bagchi, M., Roy, R., Banerjee, A. C., & Gupta, N. K. (1982) *Biochem. Biophys. Res. Commun. 104*, 89–98.

DeSa, R. J., & Wampler, J. E. (1973) *Appl. Spectrosc. 27*, 279–284.

Giblin, D. E. (1978) *Diss. Abstr. Int. B 39*, 1080–1081.

Goss, D. J., Parkhurst, L. J., Mehta, A. M., & Wahba, A. J. (1984) *Biochemistry 23*, 6522–6529.

Gupta, N. K., Woodley, C. L., Chen, Y. C., & Bose, K. K. (1973) *J. Biol. Chem. 248*, 4500–4511.

Gupta, N. K., Chetterjee, B., Chen, Y. C., & Majumdar, A. (1975) *J. Biol. Chem. 250*, 853–862.

Haugland, R. P. (1992) *Handbook of Fluorescent Probes and Research Chemicals* (Larison, K. D., Ed.) Molecular Probes, Inc., Eugene, OR.

Hellen, C. U. T., Witherell, G. W., Schmid, M., Shin, S. H., Pestova, T. V., Gil, A., & Wimmer, E. (1993) *Proc. Natl. Acad. Sci. U.S.A. 90*, 7642–7646.

Hershey, J. W. B. (1991) *Annu. Rev. Biochem. 60*, 717–755.

Jackson, R. J., Howell, M. T., & Kaminski, A. (1990) *Trends Biochem. Sci. 15*, 477–483.

Kozak, M. (1986) *Cell 44*, 283–292.

Kozak, M. (1987a) *Nucleic Acids Res. 15*, 8125–8148.

Kozak, M. (1987b) *J. Mol. Biol. 196*, 947–950.

Macejak, D. G., & Sarnow, P. (1991) *Nature 353*, 90–94.

Matasova, N. B., Mylyseva, S. V., Zenkova, M. A., Graifer, D. M., Vladimirov, S. N., & Karpova, G. G. (1991) *Anal. Biochem. 198*, 219–223.

McGhee, J. D., & von Hippel, P. H. (1974) *J. Mol. Biol. 86*, 469.

Noggle, J. H. (1985) in *Physical Chemistry on a Microcomputer*, pp 145–165, Little, Brown and Company, Boston.

Pelleteir, J., & Sonenberg, N. (1988) *Nature 334*, 320–325.

Roy, R., Nasrin, N., Ahmad, M. F., & Gupta, N. K. (1984) *Biochem. Biophys. Res. Commun. 122*, 1418–1425.

Roy, A. L., Chakrabarti, D., Datta, B., Hileman, R. E., & Gupta, N. K. (1988) *Biochemistry 27*, 8203–8209.

Schreier, M. H., & Staehelin, T. (1973) *Nature New Biol. 242*, 35–38.

Weber, G. (1975) *Adv. Protein Chem. 29*, 1–83.

Woodley, C. L., Chen, Y. C., & Gupta, N. K. (1974) *Methods Enzymol. 30*, 141–153.